December 2008
SLAC-PUB-13475

Running Shanghai Soft x-ray FEL with the EEHG scheme*

D. Xiang and G. Stupakov
SLAC National Accelerator Laboratory, Stanford, CA 94309

Abstract

With the nominal beam parameters (beam energy: 0.84 GeV, slice energy spread: 168 keV, peak current: 600 A, normalized emittance: 2 mm mrad) of the Shanghai soft X-ray Free Electron Laser (SXFEL) project, we show that using the echo-enabled harmonic generation (EEHG) scheme, 9 nm coherent soft x-ray with peak power exceeding 400 MW can be generated directly from the 270 nm seeding laser.

I. INTRODUCTION

The echo-enabled harmonic generation (EEHG) free electron laser (FEL) was recently proposed in [1] and analyzed in detail in [2]. The echo scheme has remarkable up-frequency conversion efficiency and allows for generation in the beam a high harmonic density modulation with a relatively small energy modulation.

The echo scheme uses two modulators and two dispersion sections. In general, the frequencies of the first, ω_1, and the second, ω_2, modulators can be different. The beam modulation is observed at the wavelength $2\pi / k_E$, where $ck_E = n\omega_1 + m\omega_2$, with *n* and *m* integer numbers. The first dispersion section is chosen to be strong enough, so that the energy and the density modulations induced in the first modulator is macroscopically smeared due to the slippage effect. At the same time, this smearing introduces a complicated fine structure into the phase space of the beam. The echo then occurs as a recoherence effect caused by the mixing of the correlations between the modulation in the second modulator and the structures imprinted onto the phase space by the combined effect of the first modulator and the first dispersion section. The key advantage of the echo scheme is that the amplitude of high harmonics of the echo is a very slow function of the integer numbers *n* and *m*, which is in sharp contrast to the classic HGHG scheme [3] where the amplitude of the high harmonics exponentially decays as the harmonic number increases. Due to the relatively low up-frequency conversion efficiency, in order to generate coherent soft x-rays using an UV wavelength seeding laser, multiple stages of the classic HGHG scheme are to be used [4]. The EEHG, however, allows for generation of coherent soft x-ray directly from the UV seed laser, taking advantage of its high up-frequency conversion efficiency.

We show in this paper that the SXFEL project can benefit from the EEHG scheme: the 9 nm soft x-rays with peak power exceeding 400 MW can be generated directly from the 270 nm seeding laser in a single-stage.

II. PRINCIPLES OF EEHG FEL

* Work supported by US DOE contracts DE-AC03-76SF00515.

The schematic of the EEHG FEL is shown in Fig.1.

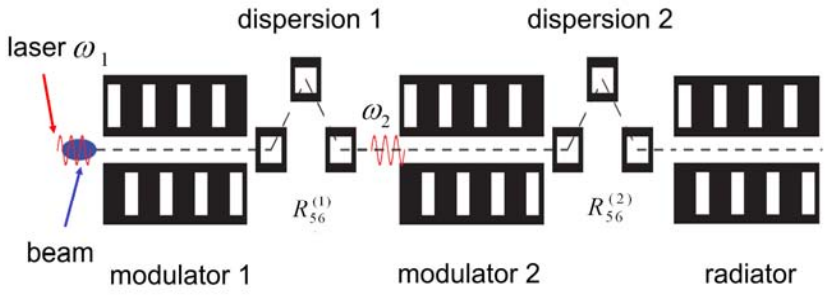

FIG.1 Schematic of the EEHG FEL. The beam is modulated in the first undulator (modulator 1) tuned at frequency ω_1 due to the interaction with the first laser beam. After passing through the first dispersion section with $R_{56}^{(1)}$, the beam energy is then modulated in the second undulator (modulator 2) tuned at frequency ω_2. Finally the beam passes through the second dispersion section $R_{56}^{(2)}$ and emits radiation in the last undulator (radiator).

The EEHG FEL consists of two modulators, two dispersion sections and one radiator. We assume an initial Gaussian beam energy distribution with an average energy E_0 and the rms energy spread σ_E, and use the variable $p = (E - E_0)/\sigma_E$ for the dimensionless energy deviation of a particle. The initial distribution function of the beam, normalized by unity, is $f(p) = N(2\pi)^{-1/2} e^{-p^2/2}$, where N is the number of electrons per unit length of the beam. Similar to the classic HGHG scheme, a laser with duration much shorter than the electron bunch length is used to modulate the beam energy in the first undulator (modulator 1). After passing through the first modulator, the beam energy is modulated with the amplitude ΔE_1, so that the final dimensionless energy deviation p' is related to the initial one p by the equation $p' = p + A_1 \sin(k_1 z)$, where $A_1 = \Delta E_1/\sigma_E$, $k_1 = \omega_1/c$, and z is the longitudinal coordinate in the beam. The distribution function after the interaction with the laser becomes $f(\zeta, p) = (2\pi)^{-1/2} \exp[-(p - A_1 \sin\zeta)^2/2]$ where we now use the dimensionless variables $\zeta = k_1 z$. Sending then the beam through the first dispersion section with the dispersion strength $R_{56}^{(1)}$, converts the longitudinal coordinate z into z', $z' = z + R_{56}^{(1)} p\sigma_E/E_0$, and makes the distribution function

$$f(\zeta, p) = \frac{N}{\sqrt{2\pi}} \exp\left[-\frac{1}{2}\left(p - A_1 \sin(\zeta - B_1 p)\right)^2\right], \qquad (1)$$

where $B_1 = R_{56}^{(1)} k_1 \sigma_E / E_0$.

The final distribution function at the exit from the second dispersion section can be easily found by applying consecutively two more transformations to (1), similar to the derivation outlined above. The resulting final distribution function is:

$$f(\zeta, p) = \frac{N}{\sqrt{2\pi}} \exp\left\{-\frac{1}{2}\left[p - A_2 \sin(K\zeta - KB_2 p + \phi)\right.\right.$$
$$\left.\left. - A_1 \sin\left[\zeta - (B_1 + B_2)p + A_2 B_1 \sin(K\zeta - KB_2 p + \phi)\right]\right]^2\right\}, \qquad (2)$$

where we now use the notation $B_2 = R_{56}^{(2)} k_1 \sigma_E / E_0$, $K = k_2 / k_1$, and A_2 is the dimensionless modulation amplitude of the beam energy in modulator 2.

From a practical point of view, using the same laser in both modulator 1 and modulator 2 is highly desirable. In this case the maximized bunching factor for the *k*-th harmonic can be written as [2],

$$b_k = \left| J_{k+1}\left[kA_2B_2\right] J_1\left[A_1\left(kB_2 - B_1\right)\right] e^{-\frac{1}{2}(kB_2 - B_1)^2} \right|, \tag{3}$$

Using the nominal parameters of the SXFEL project [5], we show below that the 30th harmonic of the seed laser can be generated with small energy modulation using the EEHG scheme. The electron beam energy of the SXFEL is 0.84 GeV and slice energy spread is about 168 keV. The wavelength of the seed laser is 270 nm. The energy modulation amplitude in modulator 1 and modulator 2 are chosen to be $A_1 = 3$ and $A_2 = 1$, respectively. The optimized dispersion strengths that maximize the bunching factor for the 30th harmonic are found to be $R_{56}^{(1)} = 7.314$ mm and $R_{56}^{(2)} = 0.240$ mm, respectively.

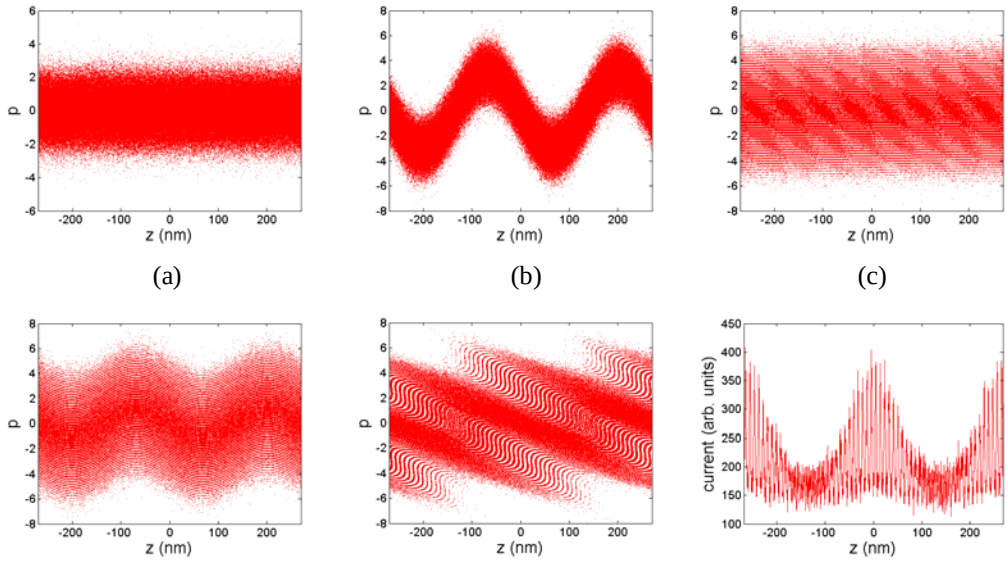

FIG.2 Longitudinal phase space evolution in the EEHG scheme. (a): phase space at the entrance to modulator 1; (b): phase space at the exit of modulator 1; (c): phase space at the exit of dispersion 1; (d): phase space at the exit of modulator 2; (e): phase space at the exit of dispersion 2; (f):current distribution at the exit of dispersion 2.

The longitudinal phase space evolution in the EEHG scheme is shown in Fig.2. After passing through the dispersion 1, we can clearly see in Fig.2c that the modulation imprinted in modulator 1 is macroscopically smeared, due to the relatively large dispersion strength. At the same time, this smearing introduces a complicated fine structure into the phase space of the beam where the separated energy bands are generated. A second laser with the same wavelength is used to modulate the beam energy in modulator 2. At the exit of modulator 2, the longitudinal phase space is shown in Fig.2d. It's worth pointing out that the inherent energy spread of each energy band is

much smaller than that of the whole beam. So for $A_2 = 1$, even though the energy modulation seen by the whole beam is at the same level of the initial local energy spread, the modulation is much larger as seen by the energy bands, taking into account the fact that the energy distribution has been chopped into many energy bands. After passing through dispersion 2, the longitudinal phase space evolves to that in Fig.2e, where we clearly see that the energy modulation for each energy band converts to density modulation. When projected to *z*-axis, we could get the current distribution for Fig.2e which is shown in Fig.2f. From Fig.2f, we could see that the current distribution contains approximately 30 spikes (separated current bands) in one wavelength region, which indicates that there is considerable component for the 30th harmonic.

Fourier transform of the current distribution gives the bunching factor at various harmonic numbers. The calculated bunching factor from Fig.2f is shown in Fig.3. For convenience of comparison, the bunching factor for the optimized classic HGHG scheme with the same energy modulation amplitude is also shown in Fig.3.

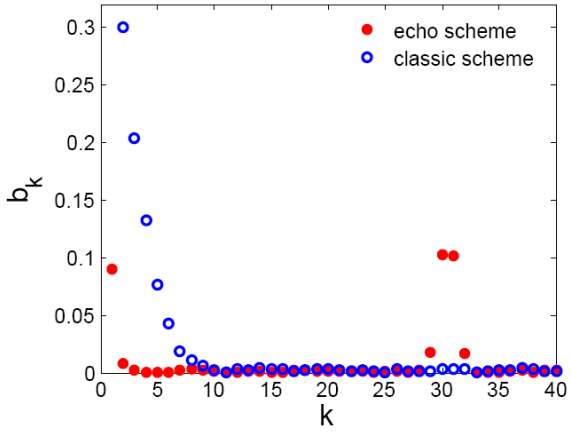

Fig.3 Comparison of the bunching factors from the EEHG scheme and that from the classic HGHG scheme.

From Fig.3 we could see for the classic HGHG scheme, the bunching factor exponentially decreases as the harmonic number increases. However, for the echo scheme, we can intentionally maximize the bunching factor for some specific harmonic number while most of the other harmonic components are effectively suppressed.

III. PERFORMANCES OF THE SXFEL USING EEHG SCHEME

The present SXFEL design uses two-stage HGHG [3-4] to generate 9 nm soft x-rays from the 270 nm seed laser. In the cascading HGHG scheme, the 6th harmonic (45 nm) of the seed laser is generated in the first stage and further used as the seed signal for the second stage. The nominal beam energy is 840 MeV, local energy spread is 168 keV, peak current is 600 A and the normalized emittance is 2 mm mrad. We show below that SXFEL could operate with EEHG scheme too.

The energy modulation and dispersion strength are chosen to be the same as described in section II to maximize the bunching factor for the 30th harmonic. The first modulator is chosen to

be 87 cm long with the undulator period length to be 5.8 cm. The input laser has a waist of 300 um and the peak power is about 60 MW. The corresponding energy modulation amplitude is $A_1 = 3$. The second modulator is 29 cm long and just has 5 undulator periods. The laser parameters are the same and the corresponding normalized energy modulation amplitude is $A_2 = 1$.

The simulation is performed with the upgraded code Genesis [6] and it consists of 3 separate runs. In the first run, the energy modulation from the 270 nm seed laser in the first modulator is simulated and the particle distribution is dumped at the exit of modulator 1. The particle distribution is imported, transported through dispersion 1 and further sent to modulator 2 for the other energy modulation. At the exit of modulator 2, the particle distribution is dumped again. Finally, the particle distribution is re-imported for the third run and the undulator period of the radiator is tuned to the 30th harmonic of the seed laser. The radiator undulator has a period length of 2.6 cm and is divided into 7 sections of 2.2 m separated by 0.3 m drift for focusing and beam diagnostics.

During the simulation, the dispersion strength and peak power of the seed laser are finely tuned to maximize the saturation power of the 9 nm radiation. The bunching factor evolution is shown in Fig.4a. The significant enhancement of the performance using the EEHG scheme is clearly seen in Fig.4b where the peak power of the 30th harmonic radiation exceeds 400 MW and the power saturates after 6 undulator sections (total magnet length is 13.2 m). The large bunching factor offered by the EEHG scheme is responsible for the initial steep quadratic growth of the power. The high peak power and short saturation length should be attributed to the initial large bunching factor and the small energy modulation in the modulators. Indeed, the local energy spread at the entrance to the radiator is only about 2.45 times the initial local energy spread.

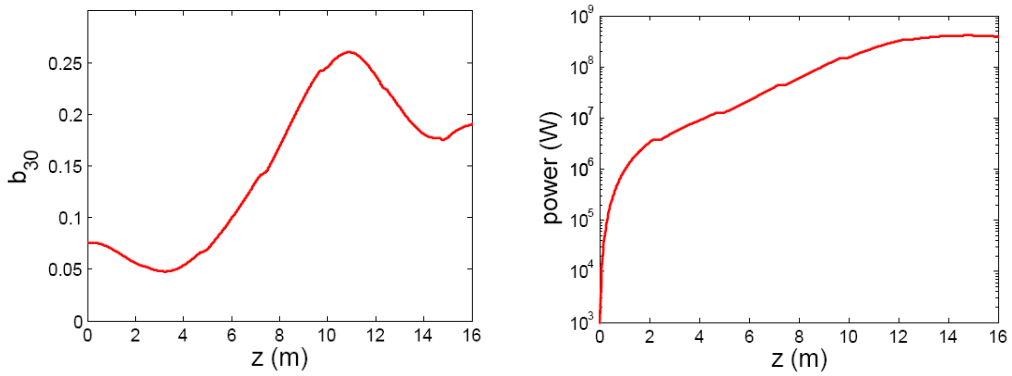

(a) (b)

Fig4. (a) Bunching factor vs radiator distance for the 9 nm radiation; (b) Peak power vs radiator distance for the 9 nm radiation.

IV. CONCLUSIONS

The EEHG FEL significantly enhances the performances of single-stage harmonic generation FEL and allows for generation of much higher harmonic. Using the nominal beam parameters of the SXFEL project, we have shown that 9 nm coherent soft x-ray with peak power exceeding 400 MW can be generated directly from the 270 nm seeding laser using the EEHG scheme. This might mitigate the jitter problem and simplify the overall design. It is worth pointing out that in our simulations and calculations, the parameters are representative rather than fully optimized design

sets. After more careful optimization, we believe there is still room for improvements. And the wake field and the sensitivity to jitter are not included in our preliminary analysis.

Acknowledgements

We thank A. Chao, Y. Ding, Z. Huang and J. Wu for helpful discussions and comments. Special thanks should be given to YD and ZH for assistance in Genesis simulations and to W. Fawley for a crosscheck simulation with GINGER. This work was supported by US DOE contracts DE-AC03-76SF00515.

---

[1] G. Stupakov, Using beam echo effect for generation of short-wavelength radiation, Preprint SLAC-PUB-13445, SLAC (2008).

[2] D. Xiang and G. Stupakov, Echo-enabled harmonic generation free electron laser, Preprint SLAC-PUB-13474, SLAC (2008).

[3] L. H. Yu, Phys. Rev. A 44, 5178 (1991).

[4] J. Wu and L.H. Yu, Nucl. Instrum. Methods Phys. Res., Sect. A 475, 104 (2001).

[5] Conceptual design report of the Shanghai Soft X-ray FEL, 2007 (in Chinese).

[6] S. Reiche, Nucl. Instrum. Methods Phys. Res., Sect. A 429, 243 (1999); S. Reiche, P. Musumeci and K. Goldammer, Proceedings of PAC07, p1269, 2007.